



First evidence of quasi-periodic magnetic intraday activity from SiO emission in the atmosphere of two Mira stars

H.W. Wiesemeyer, C. Thum, Alain Baudry, Fabrice Herpin

► To cite this version:

H.W. Wiesemeyer, C. Thum, Alain Baudry, Fabrice Herpin. First evidence of quasi-periodic magnetic intraday activity from SiO emission in the atmosphere of two Mira stars. 2008. hal-00332634

HAL Id: hal-00332634

<https://hal.science/hal-00332634>

Preprint submitted on 21 Oct 2008

HAL is a multi-disciplinary open access archive for the deposit and dissemination of scientific research documents, whether they are published or not. The documents may come from teaching and research institutions in France or abroad, or from public or private research centers.

L'archive ouverte pluridisciplinaire **HAL**, est destinée au dépôt et à la diffusion de documents scientifiques de niveau recherche, publiés ou non, émanant des établissements d'enseignement et de recherche français ou étrangers, des laboratoires publics ou privés.

First evidence of quasi-periodic magnetic intraday activity from SiO emission in the atmosphere of two Mira stars

H.W. Wiesemeyer ^{1*}, C. Thum¹, A. Baudry², F. Herpin²

¹ *Institut de Radioastronomie Millimétrique, 300 rue de la piscine, 38406 Saint Martin d'Hères, France*

² *Université de Bordeaux, Laboratoire d'Astrophysique de Bordeaux, 33000 Bordeaux, France & CNRS/INSU, UMR 5804, BP 89, 33270 Floirac, France*

* Present address: IRAM Granada, Spain

Towards the end of their lifetime, low- to intermediate mass stars undergo a phase in which they burn Helium in a shell on top of a Carbon-Oxygen core, and Hydrogen in another shell above the Helium shell¹. During this phase, where the stars appear in the Hertzsprung-Russell-Diagram in the upper asymptotic giant branch (AGB), they loose, due to a wind driven by pulsations, at least half of their mass, which forms a circumstellar envelope². The inner part of this envelope, also called extended atmosphere, is expected to bear complex magneto-hydrodynamic phenomena, due to the interaction of the wind with the previously expulsed matter and, possibly, with Jovian or terrestrial planets^{3,4}. As in the solar system, where space weather changes on timescales of hours⁵, fluctuations of the magnetic field about a mean value can be expected, but the observational evidence is still lacking. Here we show that for a narrow range of velocities the circular polarization of SiO masers, generally accepted as a tracer of the magnetic field in the extended atmosphere of AGB stars^{6,7}, varies in two AGB stars with a period of a few hours. Previous multi-epoch observations^{8,9,10} of SiO masers were neither polarimetric nor critically sampled to detect such intraday magnetic fluctuations. Because

statistically significant fluctuations are seemingly rare and localized in the extended atmosphere, they are expected to be due to a variety of phenomena. Coronal flux loops, magnetic clouds or Jovian magnetospheres³ provide suitable explanations. Our study opens the way to future observations combining intensive full polarization monitoring of SiO masers, sampling at least once per hour, with high spatial resolution. This will ultimately allow us to distinguish between the proposed scenarios and to investigate the fate of inner planetary systems around solar-type stars entering their AGB phase.

All our knowledge about the magnetism within the extended atmosphere of AGB stars relies on circular polarization measurements of SiO masers at 1.5 to 7 AU distance from the star, which typically has a radius of 0.7 to 0.8 AU. Assuming that the circular polarization is caused by the Zeeman effect in the non-paramagnetic SiO molecule, fractional circular polarizations of up to 9 % have been reported¹¹ for the v=1, J=1-0 transition (v and J are the vibrational and rotational quantum numbers, respectively), yielding magnetic flux densities of up to 100 G. These observations have been recently confirmed¹² for the spatially coincident v=1, J=2-1 masers, though resulting in lower magnetic flux densities (up to 20 G), depending on theories of maser polarization^{13,14}. In the outer envelope, H₂O and OH masers reside at ∼ 100 to 400 AU, respectively ∼ 1000 to ∼ 10.000 AU, from the star. The Zeeman effect of H₂O masers has been used¹⁵ to estimate, by extrapolation assuming a solar-type field topology, a magnetic flux density at the stellar surface of 100 G. In summary, it is now observationally evident that AGB stars can maintain a magnetic flux throughout their envelope which later may shape the gas expelled by the planetary nebulae (though its dynamical importance is still a matter of debate). Indeed, AGB stars are expected to drive a powerful dynamo at the core-envelope interface¹⁶. As for the nature of the magnetized environment in which SiO masers reside, several scenarios exist, and there are two crucial tests for them: they need to explain the observed lifetime¹⁷ of linearly polarized SiO maser features (though the

linear polarization may be of non-magnetic origin), but they also predict observable magnetic fluctuations on top of the stellar magnetosphere.

Here we provide observational evidence for short-term fluctuations of the magnetic field in the extended atmosphere of two AGB stars by simultaneous monitoring of all Stokes parameters of the $v=1, J=2-1$ maser transition of SiO with IRAM's 30m telescope. Theory of the SiO phenomenon invokes molecular excitation in dense pockets of gas and amplification of radiation in narrow tubes. Once the maser spots are formed (often distributed along arcs around the star, hereafter referred as the maser shell), they are subject to magnetospheric events known to be rapidly variable in the solar system, hence dense time sampling is important. 80 AGB stars were observed with a digital correlation polarimeter, out of which 8 objects with the strongest circular polarization were retained for a densely sampled monitoring (twice per hour). Only two AGB stars, the Mira variables V Cam and R Leo show clear evidence (Fig.1) for a quasi-periodic modulation of their fractional circular polarization p_C , at a narrow range of radial velocities of ~ 0.4 km/s centered at 7.5 km/s and 4.4 km/s. The period is 5.4 h and 6.3 h, for V Cam and R Leo, respectively (Table 1). We note that the phenomenon is both rare and localized in velocity space (and thus presumably in real space, due to the velocity structure). The likelihood of misinterpretation of a time series of Gaussian noise is $< 4\%$, respectively $< 16\%$ for the two sources (Fig. 3a, c). The observations were made in May 2006, ~ 40 days after the optical maximum of V Cam (pulsation period 522 d) and ~ 30 days after that of R Leo (pulsation period 310 d), at a phase when the SiO maser shell was expected to be in expansion⁸. The peak-to-peak variation of p_C implies a magnetic field of ~ 1 G (ref. 7, 12), if we rely on the Zeeman hypothesis to explain the origin of the Stokes V signal. It is not surprising that only the circular polarization exhibits this clear quasi-periodic fluctuation. If one considers that our telescope beam averages the polarization signal from all maser spots in the circumstellar shell, the different polarization angles – either parallel or perpendicular to the maser

shell¹⁸ – tends to strongly decrease the observed average linear polarization.

Furthermore, linear polarization can be entirely produced without magnetic fields by anisotropic pumping¹⁹ (though polarization angle swings^{8,18} by 90° are explained by changes of the magnetic field direction with respect to the propagation direction of radiation in the maser²⁰ or the Hanle effect²¹). By contrast, circular polarization is naturally enhanced in magnetized maser spots, either directly via the Zeeman splitting^{13,14}, or indirectly via birefringent conversion of linear into circular polarization due to changes of the magnetic field topology along the maser slab (ref. 22 for unsaturated masers), or due to maser saturation, rotating the quantization axis from the direction of the magnetic field to that of the radiation propagation in the maser⁶. In the latter case, pump conditions varying with time are to be generated, an event which we cannot exclude but seems unlikely on short time scales. In turn, this would produce a varying Stokes I flux density, which is not observed (Fig.1). We therefore suggest that the intraday fluctuations of p_c are of magnetic origin.

Monitoring of the Stokes I emission of SiO masers has reported variations on time scales from days²³ to years^{9,10}. To study magnetic fluctuations, the time variability of all Stokes parameters must be monitored. However, poor sampling can only be sensitive to a long-term readjustment of the magnetic field (ref. 17), while our dense sampling is sensitive to rapid magnetospheric events. As for the latter, scenarios such as (1) close binaries like the Mira AB system, (2) a global magnetic field, (3) flares and coronal loops, (4) magnetized clouds²⁴, (5) Parker instabilities in shocks forming in response to stellar pulsations²⁵, (6) Jovian magnetospheres, have been proposed, or could be proposed. In case (1), mass transfer from the AGB star to a companion may generate flares and related magnetic fluctuations, which are not necessarily located in the atmosphere of the former. V Cam and R Leo are not known for having lower mass companions, which rules out this case. As for case (2), the X-ray luminosities in two single AGB stars were found to be below the threshold expected for a dynamically

important magnetic field²⁶. This does not exclude episodic magnetic fluctuations, but in absence of a companion scenarios other than a global magnetic field need to be assumed if we want to explain the rareness of the observed fluctuations. In support to our case (3) we may suppose that the tips of flares and coronal loops directly reach the SiO maser zone. The differential rotation in the sub-photosphere of AGB stars, together with the dynamo beneath¹⁶, will lead to coronal loops (our case 3). For an upper limit, we take the rotation rate of the core from where the magnetic field emerges to be $\Omega_c \sim 10^{-5} \text{ s}^{-1}$ (ref. 16). Assuming (by solar analogy) that the size of a coronal loop corresponds to that of a super-granulation cell, this yields 0.2 AU for 400 convection cells in the stellar sub-photosphere²⁷ (in contrast to 2×10^6 for the sun), taking the stellar radius to be 1 AU. Thus, at 5 AU distance from the stellar centre, a reversal of the magnetic field component due to the flux loop should cross the line of sight of an SiO maser in one to two hours. The speed of the maser spots away from the star does not contribute to this estimate – it is lower by at least two orders of magnitude⁸. However, neither the size of the super-granules nor the stellar rotation profile are sufficiently well known to provide evidence for coronal loops crossing SiO masers, and the interaction with the pulsation-driven high-density wind certainly leads to an extremely complex physics. As in the solar system²⁸, coronal loops trigger mass ejections which subsequently form magnetic clouds (our case 4), which need about two days to cross a maser slab of 0.13 AU diameter (lower size limit from 86 GHz VLBI observations of Mira30), assuming a relative speed of 100 km/s (maser spots usually expand with a few 10 km/s, magnetic clouds in the solar system can reach a few 100 km/s). This is clearly too short to account for stable polarization features lasting for at least a month. It could, however, generate observable fluctuations with respect to the mean magnetic field.

The magnetic flux being coupled to the masering matter, the observed SiO maser lifetime must be shorter than the ambipolar diffusion timescale. The fragments forming as a consequence of Parker instabilities (our case 5, ref. 25) fulfil this requirement under the

typical conditions in the extended atmosphere of AGB stars ($T=1500$ K, hydrogen density $n_H \sim 10^{10}$ cm $^{-3}$, ionization fraction $X_i \sim 10^{-6}$, magnetic flux density $B \sim 50$ G). Since Parker instabilities arise from a local indentation orthogonal to the field lines, some short-term variations of the magnetic field component along the line of sight are also expected, and should globally affect all maser spots if the latter commonly arise from fragments formed by this mechanism.

The rapid magnetic fluctuations reported here are first rare and second strongly localized in velocity space. These findings cast doubt on the scenarios (3) and (4), coronal loops respectively magnetic clouds, expected to be ubiquitous in the stellar atmosphere. The latter finding, namely fluctuations restricted to a small velocity space, makes scenarios (2) and (5) unlikely because in such cases fluctuations of SiO features should be observed over a broad range of maser spot velocities. We therefore tend to favour scenario (6), addressing the possible presence of Jovian planets in the AGB atmosphere. Their magnetospheres and magnetotails were proposed³ for being responsible for the Zeeman effect in SiO masers, and their evaporating Galilean moons may provide an interesting reservoir to fabricate the SiO molecules⁴. Jovian magnetospheres provide a natural explanation for periodic fluctuations of maser magnetization: the rotation period of e.g. Jupiter is 9.9 hours, and its magnetic axis is tilted by 11° with respect to its rotation axis. The magnetic field, if not frozen in the maser slab, can then be expected to have a precessing component, leading to observable fluctuations of the magnetic flux density. Thus, Jovian magnetospheres provide the most attractive explanation. Even if Jovian planets in the SiO maser zone would not be rare, we need SiO masers that cross their magnetospheres, explaining why the phenomenon is rare and both restricted in velocity space and requiring a relatively strong (~ 1 G) magnetic field. As a matter of fact, R Leo shows, at the same radial velocity as our p_C fluctuation, a linear topology of spatially resolved SiO maser spots perpendicular to the archetypical ring topology of the maser shell (ref. 30), a feature

lending support to our case (6). Boldly extrapolating the rich magnetic phenomena observed in the solar system to the AGB atmospheres (where the situation is far more complex due to the high-density wind) and based on the present results, we conclude that extended and densely sampled polarization monitoring of SiO masers should satisfactorily confirm which of the scenarios (1) to (6) is predominantly at work. The case of Jovian magnetospheres will require a spatially fully resolved polarization monitoring, a difficult undertaking motivated by the rapidly increasing number of Jovian-type planets detected around main-sequence stars.

Methods summary

The IRAM 30m telescope at Pico Veleta is equipped with dual-polarization receivers. The pair operating at 3mm wavelength was tuned to the $v=1, J=2-1$ transition of SiO at 86.243 GHz, using the same local oscillator reference. The signals were analyzed with XPOL³¹, a correlation spectrometer enhanced with cross-correlation products for the signals from the orthogonally polarized receivers, at 39.0625 kHz channel spacing. The phase difference between the receivers was measured with a polarizing grid mounted in front of the cold load (at about 70 - 80 K effective temperature) of the calibration unit (ref. 31). Whenever the temperature scale was calibrated (every 10 to 20 minutes), the signal from the polarizer, with well known properties, was also observed and compared to the unpolarized calibration load at ambient temperature. The phase correction was then applied in order to attribute the measured real and imaginary part of the cross correlation product to the Stokes U parameter (in the reference frame of the telescope's Nasmyth focus) and the Stokes V parameter (positive for a RHC polarized signal, according to IAU convention). The polarized calibration load fills the receiver beam, whereas the SiO masers are unresolved. The cross-correlation products therefore remain sensitive to the different phase apodization across the receivers' aperture when an unresolved source is observed. The corresponding phase error results in a leakage of the

Stokes U signal into Stokes V, a subtle effect only worth worrying about when Stokes U is strong (which is the case here). The scaled ($\sim 3\%$) copy of the Stokes U signal contaminating the measured circular polarization can be removed, since it is subject to the parallactic rotation of the polarization vector, which easily shows in the data. The remaining Stokes V signal is intrinsic, the contribution of the telescope and the receiver cabin optics being negligible ($-0.03 \pm 0.12\%$ on the optical axis). Due to the irregular sampling, a determination of the spectral power density (SPD) of the time series using Fourier transform techniques yields poor results, and preference was given to the SPD estimate provided by the Lomb technique^{32,33}, which only uses the measured data without any prior interpolation to a regular sampling function. Our detection of quasi-periodic fluctuations of p_C passed three critical tests. First, we note that the Lomb periodogram of Stokes U, after subtraction of the stationary linear polarization feature, does not show any periodic signal (Figs. 3b, d). Second, the oscillation of p_C was tested against the null hypothesis that the data are not periodic, but random noise with a Gaussian distribution; this test yields the false-alarm probability given in Table 1 and Fig. 3. Third, because a restricted number of random samples cannot be strictly Gaussian, a Monte-Carlo simulation, with random samples contemporaneous with the observed features, shows, for 100.000 runs, that only 0.28 % of the Lomb periodograms mimic a periodic signal with $\leq 4\%$ false-alarm probability (V Cam), respectively 2.9 % a periodic signal with $\leq 16\%$ false-alarm probability (R Leo). We therefore conclude that it is unlikely (for V Cam extremely unlikely) that random noise creates the observed fluctuations. If they were produced by an oscillation of the telescope tracking, moving the polarized sidelobes across the line-of-sight towards the source, all velocity channels would show fluctuations with the same period, which clearly is not observed and can therefore be safely excluded.

1. Herwig, F. Evolution of Asymptotic Giant Branch Stars. *Ann.Rev.Astron.Astrophys.* **43**, 435-479 (2005).
2. Habing, H.J. Circumstellar envelopes and Asymptotic Giant Branch stars. *Astron.Astrophys.Rev.* **7**, 97-207 (1996).
3. Struck, C., Cohenim, B.E. & Willson, L.A. Models of Planets and Brown Dwarfs in Mira Winds. *Astrophys.J.* **572**, L83-L86 (2002).
4. Struck-Marcell, C. SiO masers in late-type giant stars - Jovian planets engulfed. *Astrophys.J.* **330**, 986-991 (1988).
5. Prangé, R., Pallier, L., Hansen, K.C., Howard, R., Vourlidas, A., Courtin, R. & Parkinson, C. An interplanetary shock traced by planetary auroral storms from the Sun to Saturn. *Nature* **432**, 78-81 (2004).
6. Nedoluha, G.E. & Watson, W.D. Intensity-dependent circular polarization and circumstellar magnetic fields from the observation of SiO masers. *Astrophys.J.* **423**, 394-411 (1994).
7. Elitzur, M. Polarization of Astronomical Maser Radiation. III. Arbitrary Zeeman Splitting and Anisotropic Pumping. *Astrophys.J.* **457**, 415-450 (1996).
8. Diamond, P.J. & Kemball, A.J. A Movie of a Star: Multiepoch Very Long Baseline Array Imaging of the SiO Masers toward the Mira Variable TX Cam. *Astrophys.J.* **599**, 1372-1382 (2003).
9. Pardo, J.R., Alcolea, J., Bujarrabal, V., Colomer, F., del Romero, A. & de Vicente, P. ^{28}SiO $v=1$ and $v=2$, $J=1-0$ maser variability in evolved stars. Eleven years of short spaced monitoring. *Astron.Astrophys.* **424**, 145-156 (2004).
10. Kang, J. et al. Time Monitoring Observations of SiO $J = 2-1$ and $J = 3-2$ Maser Emission toward Late-Type Stars. *Astrophys.J.Suppl.* **165**, 360–385 (2006).

11. Barvainis, R., McIntosh, G. & Predmore, C.R. Evidence for strong magnetic fields in the inner envelopes of late-type stars. *Nature* **329**, 613-615 (1987).
12. Herpin, F., Baudry, A., Thum, C., Morris, D., Wiesemeyer, H. Full polarization study of SiO masers at 86 GHz. *Astron.Astrophys.* **450**, 667-680 (2006).
13. Deguchi, S. & Watson, W.D., Circular polarization of astrophysical masers due to overlap of Zeeman components. *Astrophys.J.* **300**, L15-L18 (1986).
14. Elitzur, M. in *Astrophysical Spectropolarimetry* (eds. Trujillo-Bueno, J., Moreno-Insertis, F. & Sánchez, F.) 225-264 (Cambridge University Press, Cambridge UK, 2002).
15. Vlemmings, W.H.T., Diamond, P.J. & van Langevelde, H.J. Circular polarization of water masers in the circumstellar envelopes of late type stars. *Astron.Astrophys.* **394**, 589-602 (2002).
16. Blackman, E.G., Frank, A., Markiel, J.A., Thomas, J.A. & van Horn, H.M. Dynamos in asymptotic-giant-branch stars as the origin of magnetic fields shaping planetary nebulae. *Nature* **409**, 485-487 (2001).
17. Glenn, J., Jewell, P.R., Fourre, R. & Miaja, L. A Polarization Survey of SiO Maser Variability in Evolved Stars. *Astrophys.J.* **588**, 478-485 (2003).
18. Desmurs, J.F., Bujarrabal, V., Colomer, F., Alcolea, J. VLBA observations of SiO masers: arguments in favor of radiative pumping mechanisms. *Astron.Astrophys.* **360**, 189 – 195 (2000).
19. Western, L.R. & Watson, W.D. Linear polarization of astronomical masers by anisotropic pumping and its enhancement due to geometry. *Astrophys.J.* **275**, 195-200 (1983).
20. Goldreich, P., Keeley, D.A. & Kwan, J.Y. Astrophysical Masers. II. Polarization Properties. *Astrophys.J.* **179**, 111 (1973).

21. Asensio Ramos, A., Landi Degl'Innocenti, E. & Trujillo Bueno, J. Dichroic masers due to radiation anisotropy and the influence of the Hanle effect on the circumstellar SiO polarization. *Astrophys.J.* **625**, 985-995 (2005).
22. Wiebe, D.S. & Watson, W.D. A Non-Zeeman Interpretation for Polarized Maser Radiation and the Magnetic Field at the Atmospheres of Late-Type Giants. *Astrophys.J.* **503**, L71 (1998).
23. Pijpers, F.P., Pardo, J.R. & Bujarrabal, V. Short time scale monitoring of SiO sources. *Astron.Astrophys.* **286**, 501-507 (1994).
24. Soker, N. & Kastner, J.H. Magnetic Flares on Asymptotic Giant Branch Stars. *Astrophys.J.* **592**, 498-503 (2003).
25. Hartquist, T.W. & Dyson, J.E. The origin of strong magnetic fields in circumstellar SiO masers. *Astron.Astrophys.* **319**, 589-592 (1997).
26. Kastner, J.H. & Soker, N. Constraining the X-ray luminosities of asymptotic giant branch stars: TX Camelopardis and T Cassiopeiae. *Astrophys.J.* **608**, 978-982 (2004).
27. Schwarzschild, M. On the scale of photospheric convection in red giants and supergiants. *Astrophys.J.* **195**, 137-144 (1975).
28. Burlaga, L.F. et al. A magnetic cloud and a coronal mass ejection. *Geophys.Res.L.* **9**, 1317-1320 (1982).
29. Phillips, R.B. & Boboltz, D.A. 86 GHz Masers toward Mira. *Astron.J.* **119**, 3015-3018 (2000).
30. Cotton, W.D., Perrin, G. & Lopez, B. VLBA SiO observations of bright O-rich AGB stars. *Astron.Astrophys.* **477**, 853-863 (2008).
31. Thum, C., Wiesemeyer, H., Paubert, G., Navarro, S. & Morris, D. XPOL – the correlation polarimeter at the IRAM 30m telescope. *Publ.Astr.Soc.Pac.* **120**, 777-790 (2008).

32. Press, W.H., Teukolsky, S.A., Vetterling, W. & Flannery, B.P. Numerical Recipes in C, 575-584 (Cambridge University Press, Cambridge UK, 1994).
33. Lomb, N.R. Least-squares frequency analysis of unequally spaced data. *Astrophys.Space.Sc.* **39**, 447-462 (1976).

Acknowledgements Based on observations with the IRAM 30m telescope. IRAM is supported by INSU/CNRS (France), MPG (Germany) and IGN (Spain). Gabriel Paubert supported by the IRAM backend group built VESPA which provides simultaneous measurements of all Stokes parameters. We used the valuable optical lightcurves of the AAVSO (<http://www.aavso.org>) and acknowledge support from the telescope staff.

Author Information Correspondence and requests for materials should be addressed to H.W. (wiesemeyer@iram.es).

Figure 1 | Spectra of total power (Stokes I, i.e. polarized plus unpolarized) flux density and fractional circular polarization. Grey-shaded histogram: Stokes I flux density in Jansky vs. v_{lsr} (the radial velocity with respect to the local standard of rest). Dots with errorbars: fractional circular polarization p_c , in % with respect to Stokes I. Top **(a)**: Mira star V Cam. Bottom **(b)**: Mira star R Leo.

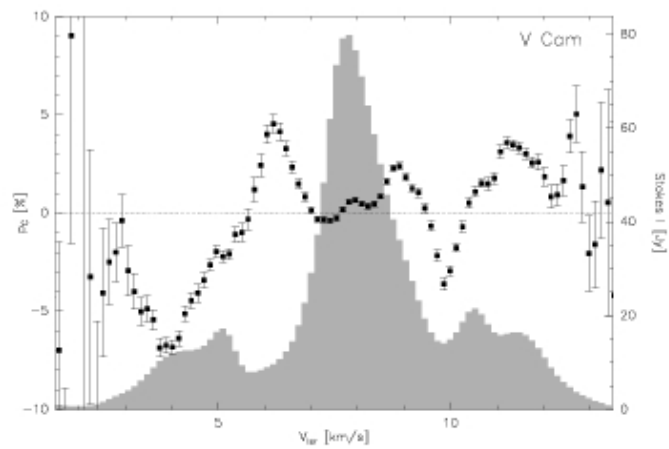
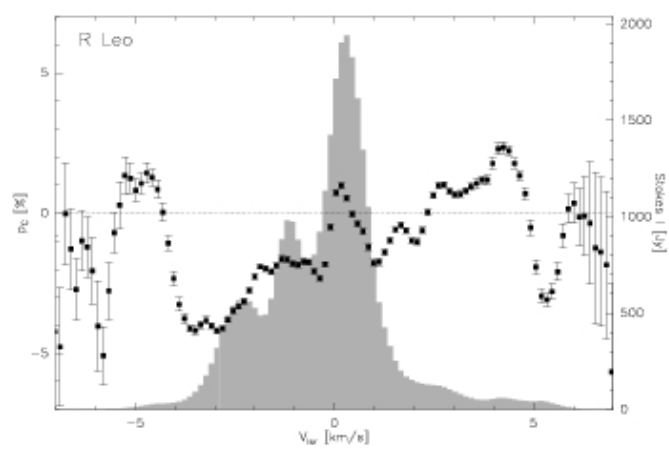
Figure 2 | Time series of polarization measurements. From top to bottom: time series of Stokes I in Jansky, the fractional polarizations p_L (linear) and p_C (circular), and the polarization angle (i.e. the position angle of linear polarization, in degree E from N), for the SiO maser spots from V Cam at $v_{\text{lsr}} = 7.5 \text{ km/s}$ (left, **a**) and R Leo at $v_{\text{lsr}} = 4.4 \text{ km/s}$ (right, **b**).

Figure 3 | Lomb periodograms of the polarization time series. Estimate of the spectral power density of the polarization time series by least-square fits of its harmonic contents (Lomb periodogram^{32,34}), normalized by the variance of the samples. **(a)** Lomb periodogram of the fractional circular polarization p_C of V Cam at $v_{\text{lsr}} = 7.5 \text{ km/s}$, **(b)** same for the residuals of Stokes U (normalized by Stokes I, after subtraction of the stationary linear polarization). **(c)** and **(d)**: as (a) respectively (b) but for R Leo at $v_{\text{lsr}} = 4.4 \text{ km/s}$. The horizontal dashed lines indicate the spectral powerdensity at which a periodic signal can be mimicked by Gaussian noise with a probability given by the labels (“false alarm probability”). For a given source, the plot scale for the Lomb periodograms of p_C and the Stokes U residuals is the same, to make the comparison of the significance of the peaks easier.

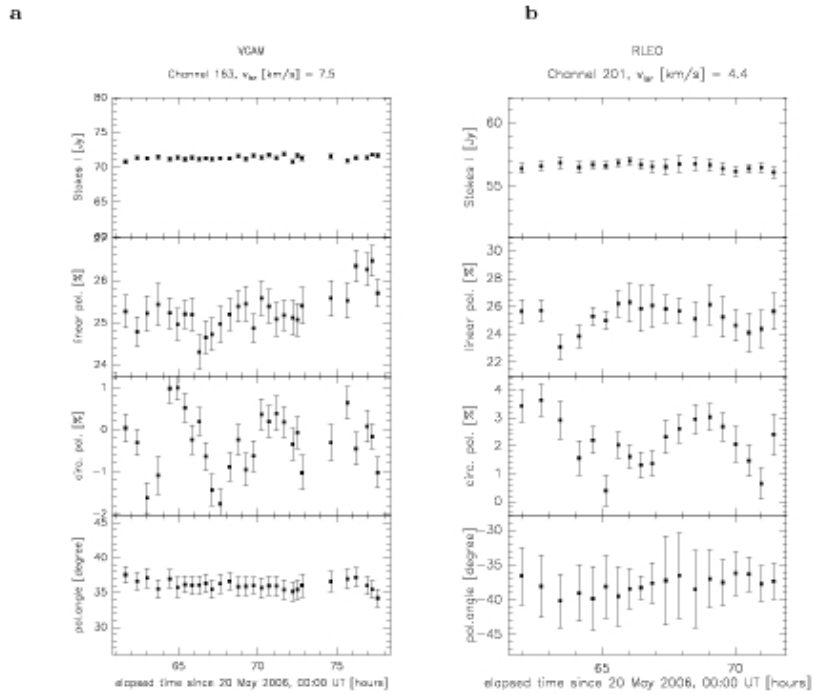
Table 1 Observational Results

	V Cam	R Leo
Phase of optical lightcurve ⁽¹⁾	0.08	0.10
Oscillation period of circular polarization	(5.4±0.1) h	(6.3 ± 0.3) h
False-alarm probability ⁽²⁾	4 %	16 %
radial velocity of maser spots ⁽³⁾	7.5 km/s	4.4 km/s
Mean circular polarization	-0.3 %	+2.0 %
Mean magnetic flux density in maser ⁽⁴⁾	~ 100 mG	~ 1 G
Peak-to-peak variation of fractional polarization	2.8 % = 5.6 σ_{rms}	3.7% = 7.4 σ_{rms}
Fluctuation of magnetic field ⁽⁴⁾	~ 1 G	~ 1 G

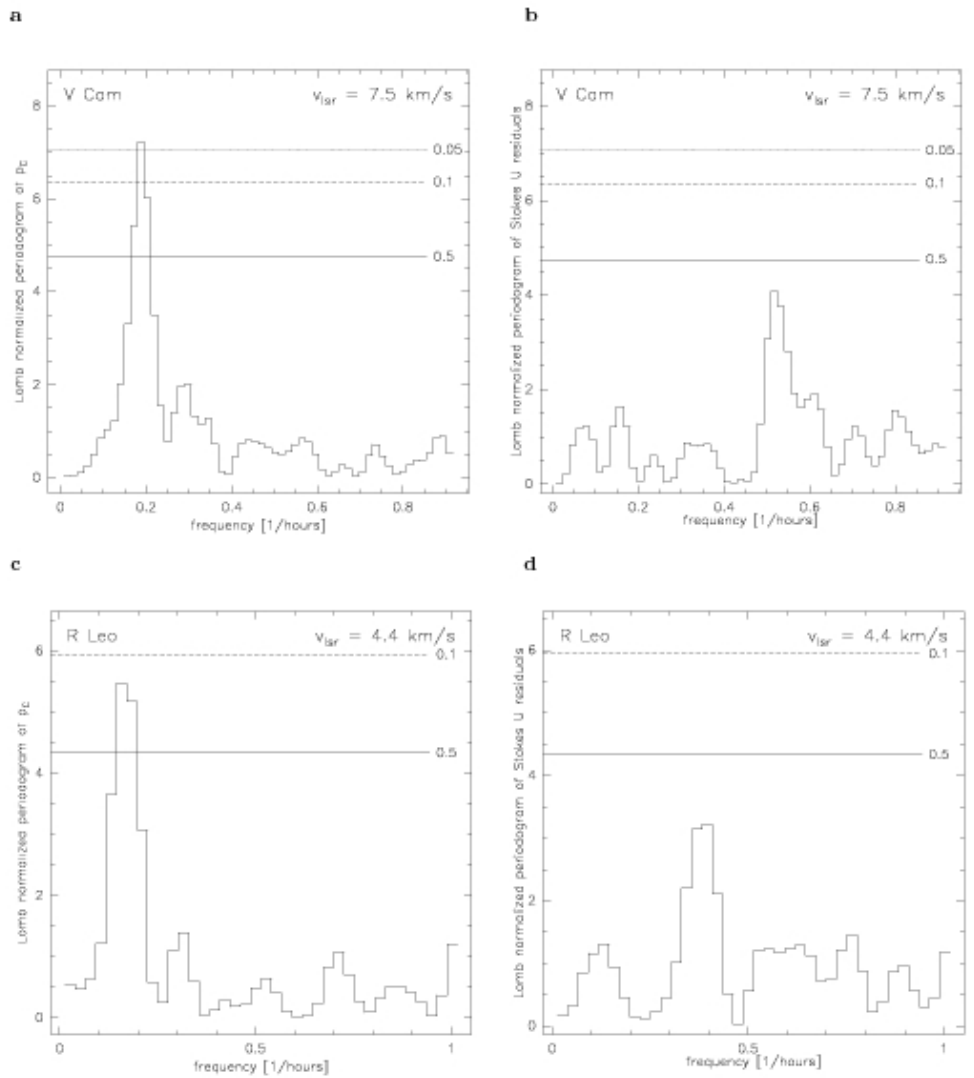
⁽¹⁾ With respect to the maximum of the optical lightcurve, ⁽²⁾ with respect to the null hypothesis (data are Gaussian noise), ⁽³⁾ with respect to the local standard of rest , ⁽⁴⁾ order of magnitude estimate based on the Zeeman hypothesis, and for a linewidth of 1 km/s (ref. 7, 12).

a**b**

H. Wiesemeyer, Figure 1



H. Wiesemeyer, Figure 2



H. Wiesemeyer, Figure 3